# A MECHANISTIC EXPERIMENT ON STRESS CORROSION CRACKING PROCESS IN 8090 ALUMINUM-LITHIUM ALLOY

**Shuhei Osaki, Makio Iino, and Ken Kaminishi**
Faculty of Engineering, Yamaguchi University
Tokiwadai Ube 755 Japan

ABSTRACT The stress corrosion cracking (SCC) behaviors of a 8090 Al-Li alloy in the two underaging conditions UA1 and UA2 are investigated and compared with that of the conventional 7075-T6 alloy. A notched plate specimen was used for the SCC test in 3.5% sodium chloride solution, subjected to a bending load in the S-L orientation. The stress distribution and associated development of plastic zone at the notch root were determined by elasto-plastic FEM analysis. Based on experiments of SCC response with to the applied load, stress analysis and fractographic observations, a potential SCC mechanism in the 8090 alloy is discussed. It is proposed that both hydrogen embrittlement(HE) and local anodic dissolution(AD) mechanisms operate: under the early stage of aging UA1, HE plays a major role as with 7075-T6, while under the stage of near peak-aging UA2 , AD plays an important role.

Keywords: *Al-Li alloy, stress corrosion cracking, hydrogen embrittlement, plastic zone, intergranular corrosion*

## 1. INTRODUCTION

Aluminum-lithium alloys are stronger than conventional aluminum alloys with higher elastic moduli and lower density. Thus they are promising structural materials for aerospace applications which require an ultimate weight-saving. For any structural materials, a balance among strength, toughness and environmental strength should always be taken into consideration to be optimized. Age-hardened Al-Li alloys unfortunately exhibit a reduced fracture toughness[1] and a comparable susceptibility to stress corrosion cracking(SCC) with conventional aluminum alloys[2].

Although SCC characteristics of Al-Li alloys have been studied fairly in detail concerning with the influence of microstructural[2,3] and environmental factors[4,5], there have been limited work reported from mechanistic aspects. The results of such factors on SCC response appear to be often discrepant depending on alloy conditions and testing methods. SCC mechanism of Al-Li alloys has not been fully understood, even though two models have been proposed as possible mechanisms, namely hydrogen embrittlement (HE) [6,7]and local anodic dissolution(AD)[4,8].

With the above-mentioned background, the objective of this work is to examine SCC response on a notched specimen of Al-Li alloy 8090 and a conventional alloy 7075-T6 for comparison, together with analyzing stress-strain distribution by FEM, and to discuss a potential SCC mechanism of the 8090 alloy.

Table 1 Chemical composition of alloys tested(mass%).

| Alloy | Li | Cu | Mg | Fe | Si | Zr | Ti | Al |
|---|---|---|---|---|---|---|---|---|
| 8090 | 2.61 | 1.25 | 0.87 | 0.05 | 0.03 | 0.12 | 0.02 | bal. |

| Alloy | Si | Fe | Cu | Mn | Mg | Cr | Zn | Ti | Al |
|---|---|---|---|---|---|---|---|---|---|
| 7075 | 0.08 | 0.17 | 1.55 | 0.03 | 2.49 | 0.21 | 5.53 | 0.04 | bal. |

Table 2 Mechanical properties in the S direction of alloys tested.

| Alloy | Yield strength $\sigma_{ys}$ (MPa) | Tensile strength $\sigma_B$ (MPa) | Elongation $\delta$ (%) | Young's modulus E (GPa) |
|---|---|---|---|---|
| 8090-UA1 | 303 | 437 | 9.0 | 78.9 |
| 8090-UA2 | 368 | 476 | 5.1 | 78.9 |
| 7075-T6 | 486 | 560 | 5.0 | 71.4 |

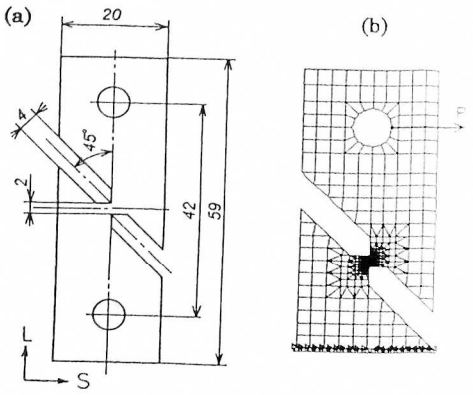


**Fig.1(a)**A notched plate specimen and **(b)**mesh used in stress analysis.

## 2. EXPERIMENTAL PROCEDURE

The materials used are hot-rolled plates of Al-Li alloy 8090 and a conventional alloy 7075. The chemical compositions of these alloys are shown in **Table 1**. Alloy 8090 is melted in a vacuum furnace and cast into ingots with a section of 300x1000mm. The ingot are homogenized in two stages, followed by hot-rolling to plates with thickness of 22mm. The alloy plate is solution treated, cold water quenched and cold worked by 2%. Subsequently the plate is subjected to the aging treatment in underaging conditions at 433K for 28.8ks(UA1) and 345.6ks(UA2). The alloy 7075 is subjected to a T6 temper of 393K-86.4ks.

For SCC tests, notched plate specimens shown in **Fig.1(a)** are machined from the plates in the S-L orientation. A horizontal load is applied as shown in Fig1(b), with the lower part of the specimen being fixed, which leads to a bending stress at the notched section, generating tension at the upper notch root and compression at the lower one. Before testing, specimens are cleaned by dipping in 10%NaOH solution for 2 min. at 303K, followed by rinsing and drying. For supply of test solution into the upper notch a small rubber pipes are attached to the specimen using insulating tape and adhesive. SCC tests are carried out under constant load conditions at room temperature. The test environment is total immersion in 3.5%NaCl solution with a supply rate of 2.3ml/ks. By measuring the change of displacement at the loading point of the specimen during tests, progress of SCC and thus time to rupture are determined.

The stress state and associated development of plastic zone at the notch root of the specimen is analyzed by elasto-plastic FEM . The analysis is performed using the mesh shown in Fig.1(b) and based on the true stress-strain relations simulating tensile properties in the S direction listed in Table 2.

## 3. RESULTS AND DISCUSSION

### 3.1 Analysis of stress-strain distribution

The load-displacement relation was measured by a mechanical testing, and compared with elasto-plastic FEM results. A fairly good agreement was confirmed to be found. The elastic limit load (P0) was defined as the load when the maximum value of Mises equivalent stress ($\sigma_{eq}$) at the notch root comes up to the yield stress ($\sigma_{ys}$). Thus defined P0 for 8090-UA1, -UA2 and 7075-T6 were computed to give 23.8, 28.9 and 51.5N respectively. The stress state was computationally determined in similar manner under a load level Pi ( i=1,2 ···) listed in Table 3. For example, Fig.2 is a result on 8090-UA2 specimen, showing development of plastic zone at the notch root, where the line drawings present elasto-plastic boundaries under various loads. The plastic zone is found to extend initially in the horizontal (X) direction, and then in the lower left direction of around 45° with increase in the load. Fig.3 exhibits development of hydrostatic stress field on 8090-UA1 specimen.

Table 3 Elastic limit load P0 and applied load Pi under which stress analysis and SCC tests are carried out.

| Load (N) | 8090-UA1 | 8090-UA2 | 7075-T6 |
|---|---|---|---|
| P0 | 23. 8 | 28. 9 | 51. 5 |
| P1 | 43. 0 | 43. 0 | 63. 3 |
| P2 | 54. 8 | 54. 8 | 79. 0 |
| P3 | 62. 6 | 62. 6 | 90. 8 |
| P4 | 70. 5 | 70. 5 | 102. 5 |
| P5 | 82. 2 | 82. 2 | 110. 4 |
| P6 | – | 94. 0 | 122. 2 |

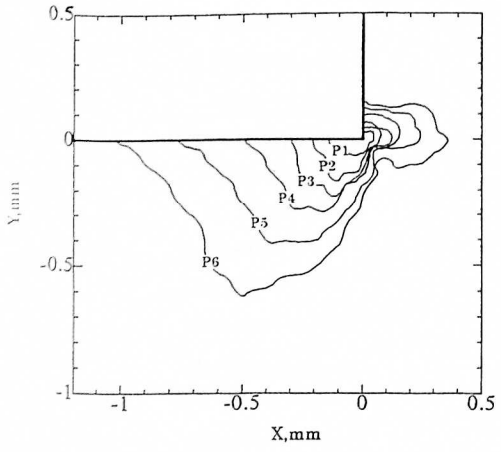


Fig.2 Development of plastic zone at the notch root of 8090-UA2 specimen.

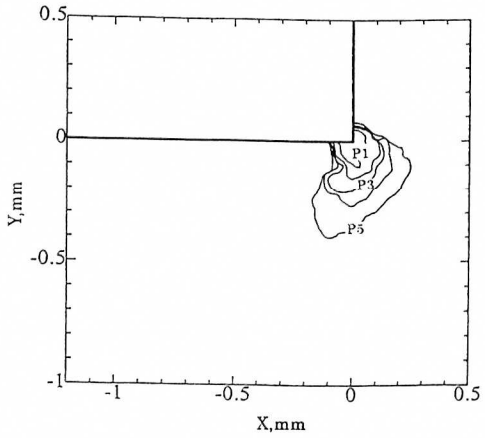


Fig.3 Development of hydrostatic stress at the notch root of 8090-UA1 specimen.

### 3.2 SCC response

The relation between load and SCC rupture time for the reference alloy 7075-T6 is presented in Fig.4. The 7075-T6 in the S-L orientation was so susceptible to SCC as commonly known that the theshold load $P_{SCC}$, defined as SCC rupture occurs in 30days, was found to be in a low level around 51.5N. This value is in close agreement with the analyzed elastic limit load, P0, below which no plastic yielding takes place at the notch root, suggesting that SCC of this alloy results from hydrogen embrittlement induced by plastic deformation[9,10].

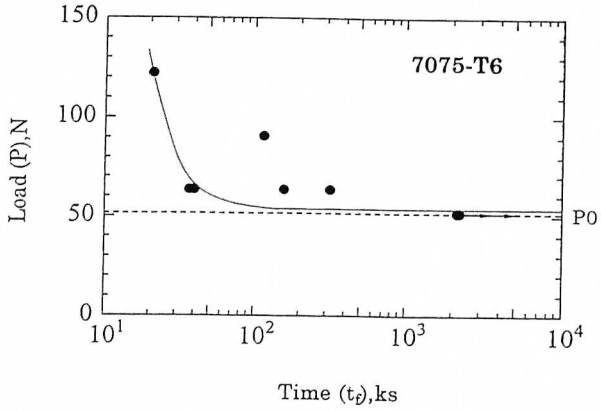


**Fig.4** The relation between load and SCC rupture time for alloy 7075-T6.

Fig.5 (a) and (b) show SCC test results for alloy 8090 aged to UA1 and UA2 conditions respectively. $P_{SCC}$ of the alloy under the UA1 condition appears to be in the neighborhood of 23.8N, which can be regarded as P0 of its alloy specimen. For the alloy under UA2 condition, on the other hand, $P_{SCC}$ is around 62.6N, a significantly higher level than P0. Thus the Al-Li alloy 8090-UA2 under near peak-aged condition will have a higher SCC resistance than the conventional alloy 7075-T6, though the yield strength is practically lower.

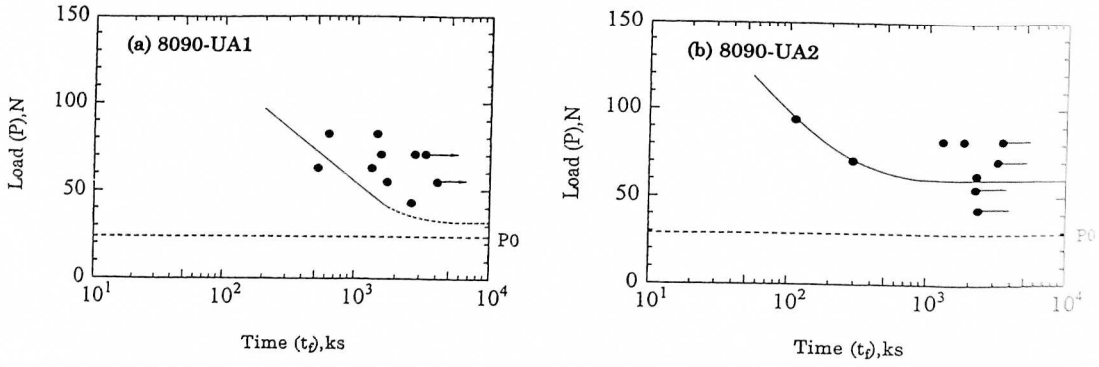


**Fig.5** The relation between load and SCC rupture time for alloy 8090 aged to (a)UA1 and (b)UA2.

3.3 Fractography

According to microscopic observations of the SCC ruptured 7075-T6 specimen, there is no indication of pitting or intergranular corrosion attack on the notch bottom face. SEM examinations of SCC fracture surface revealed a typical intergranular brittle feature with little traces of corrosion attack. These fractographic observations together with the above-mentioned SCC occurrence concurrent with the development of plastic zone at notch root indicate that the SCC of 7075-T6 is caused by HE due to hydrogen transported to the grain boundaries by means of mobile dislocations[9].

The metallographic examination of the SCC ruptured 8090-UA1 specimen under the load P4 revealed several intergranular microcracks generated just behind the fracture surface, as shown in Fig.6. The site of microcracks initiation appeared to correspond with the front of zone of elevated hydrostatic stress below the notch root, as demonstrated in Fig.3. And the UA1 specimen is characterized by the absence of development of localized corrosion attack. Thus, it would be suggested that HE plays a major role in the SCC of the 8090-UA1.

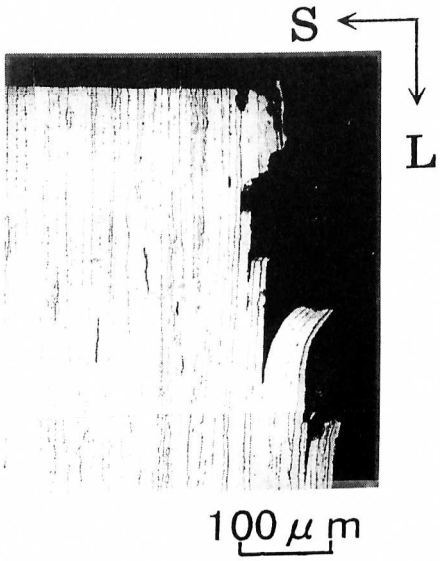


Fig.6 Intergranular microcracks generated just behind fracture surface of SCC ruptured 8090-UA1 specimen.

The 8090-UA2 specimens, on the other hand, revealed different features from the UA1 specimen. Fig.7(a)is an example of metallographic examination showing the notch bottom face of the UA2 specimen ruptured under the load P6. According to the result of stress analysis shown in Fig.2, the plastic zone at the notch bottom face under the present loading condition has been estimated to spread over the width of approximately 0.9mm in the X direction. Within the plastic zone, stimulated generation of intergranular corrosion was observed(Fig.7(c)) , while in the surrounding elastic area a reduced corrosion attack took place(Fig.7(b)). The intergranular SCC fracture surface, as shown in SEM micrograhps, was accompanied by traces of pitting attack, so that the evidence of anodic dissolution along the grain boundaries was apparent. Originally the alloy 8090 showed susceptibility to intergranular corrosion, which increased with aging time and became highest under the peak-aging condition. The intergranular corrosion would be caused by Cu-bearing S'($Al_2CuMg$) precipitates at grain boundaries, leaving a Cu-depleted anodic zone there as a pathway for preferential attack[4]. These results then show that a strain-assisted AD process along the grain boundaries play an important role in the SCC of the 8090-UA2.

Thus, based on the present experiments it is proposed that in the 8090 Al-Li alloy both HE and AD mechanisms operate: in the early stage of aging UA1, HE plays a major role, and in the stage of near peak-aging UA2 , a mechanisms cross-over takes place, AD playing a more important role.

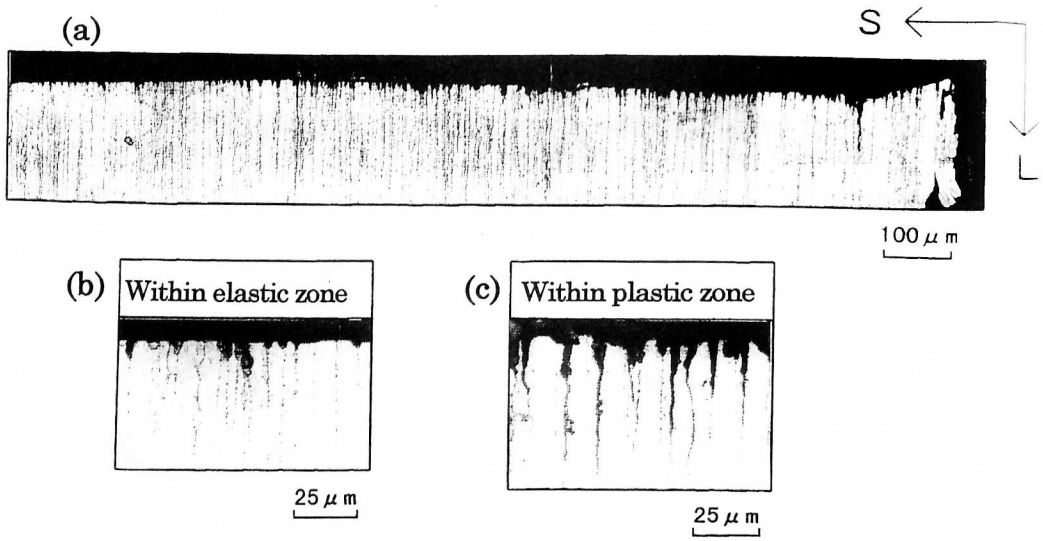


**Fig.7** Micrographs showing (a)the notch bottom face of 8090-UA2 specimen SCC ruptured under load P6. (b) A reduced corrosion attack within the elastic area and (c) intergranular corrosion within the plastic zone.

## 4.. CONCLUSIONS

Based on experiments of SCC response using a notched plate specimen, stress analysis and fractographic observations, it is supported that SCC of the reference alloy 7075-T6 is caused by hydrogen embrittlement(HE) induced by plastic deformation. As for the 8090 alloy, on the other hand, it is proposed that both HE and local anodic dissolution(AD) mechanisms operate: under the early stage of aging UA1, HE plays a major role as with 7075-T6, while under the stage of near peak-aging UA2 , AD plays an important role.

## REFERENCES

[1]K.T.Venkateswara Rao and R.O.Ritchie:Mater.Sci.Tech.,5(1989),882.
[2]N.J.H.Holroyd,A.Gray,G.M.Scamans and R.Hermann:Aluminium-Lithium Alloys III (eds.C.Baker,P.J.Gregson,S.J.Harris and C.J.Peel),The Inst. of Metals,(1986),310.
[3]E.I.Meletis:Mater.Sci.Eng.,93(1987),235.
[4]F.D.Wall and G.E.Stoner:Corr.Sci.,39(1997),835.
[5]R.G.Buchheit,F.D.Wall,G.E.Stoner and J.P.Moran:Corr.,51(1994),417.
[6]R.Balasubramaniam,D.J.Duquette and K.Rajan:Acta metall.Mater.,39(1991),2597.
[7]Z.F.Wang,Z.Y.Zhu,Y.Zhang and W.Ke:Metall.Trans.,23A(1992),3337.
[8]R.C.Dorward and K.R.Hasse:Corr.,44(1988),932.
[9]J.Albrecht,I.M.Bernstein and A.W.Thompson :Metall.Trans.,13A(1982),811.
[10]S.Osaki,M.Iino,and M.Utsue:J.Jpn.Inst.Light Metals,47(1997),370.